Journal of Advanced Research 41 (2022) 1–12

Contents lists available at ScienceDirect

Journal of Advanced Research

journal homepage: www.elsevier.com/locate/jare

Original Article

The ubiquitin-specific protease 8 antagonizes melatonin-induced endocytic degradation of MT_1 receptor to promote lung adenocarcinoma growth

Qianhui Sun [a,b,1], Jinrui Zhang [a,1], Xiaoxi Li [c,1], Guoheng Yang [a], Shaoxuan Cheng [a], Dong Guo [a], Qingqing Zhang [d], Feng Sun [e], Feng Zhao [f], Dian Yang [a], Shanshan Wang [a], Taishu Wang [a], Shuyan Liu [a], Lijuan Zou [a,*], Yingqiu Zhang [a,*], Han Liu [a,*]

[a] Second Affiliated Hospital, Institute of Cancer Stem Cell, Dalian Medical University, Dalian, China
[b] Clinical Laboratory, The Third People's Hospital of Dalian, Dalian Medical University, Dalian, China
[c] Central Laboratory, Cancer Hospital of China Medical University, Liaoning Cancer Hospital & Institute, Shenyang, China
[d] Department of Pathology, College of Basic Medical Sciences, Dalian Medical University, Dalian, China
[e] College of Life Science, Liaoning Normal University, Dalian, China
[f] Department of Cell Biology, College of Basic Medical Sciences, Dalian Medical University, Dalian, China

HIGHLIGHTS

- Melatonin can induce the downregulation of the MT_1 receptor.
- MT_1 receptor internalization incurred by melatonin follows the canonical endolysosomal pathway.
- The ubiquitin-specific protease 8 antagonizes the endocytic degradation of the MT_1 receptor.
- The suppression of ubiquitin-specific protease 8 potentiates the cancer-inhibitory effects of melatonin *in vitro*.
- Combination of USP8 inhibition and melatonin treatment effectively deters tumor growth in xenograft mouse models.

GRAPHICAL ABSTRACT

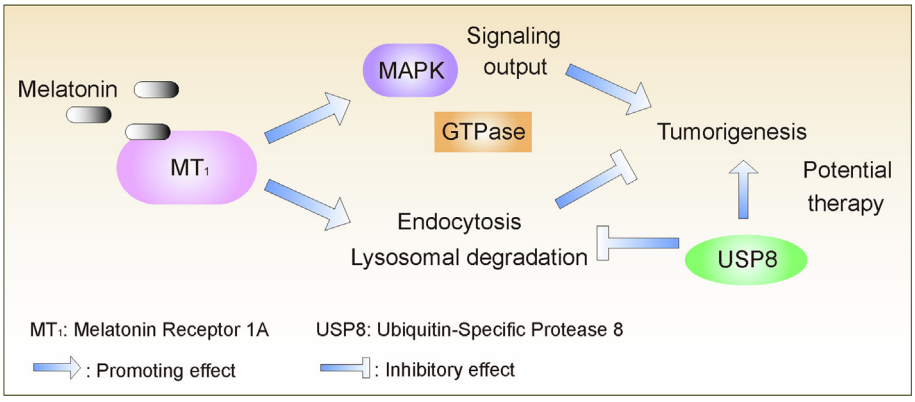

ARTICLE INFO

Article history:
Received 12 May 2021
Revised 24 January 2022
Accepted 27 January 2022
Available online 1 February 2022

Keywords:
Melatonin
MT_1
USP8

ABSTRACT

Introduction: The human genome encodes two melatonin receptors (MT_1 and MT_2) that relay melatonin signals to cellular interior. Accumulating evidence has linked melatonin to multiple health benefits, among which its anticancer effects have become well-established. However, the implications of its receptors in lung adenocarcinoma have so far remained incompletely understood.
Objectives: This study aims to investigate the response of the MT_1 receptor to melatonin treatment and its dynamic regulation by ubiquitin-specific protease 8 (USP8) in lung adenocarcinoma.
Methods: The mRNA levels of MT_1 and MT_2 receptors were analyzed with sequencing data. The expression and localization of the MT_1 receptor with melatonin treatment were investigated by immunoblotting, immunofluorescence and confocal microscopy assays. Endocytic deubiquitylases were screened to identify MT_1 association. The effects of USP8 were assessed with shRNA-mediated knockdown and small

Peer review under responsibility of Cairo University.

* Corresponding authors at: Second Hospital of Dalian Medical University, 467 Zhongshan Road, Shahekou District, Dalian, Liaoning Province, China. (L Zou). Institute of Cancer Stem Cell, Dalian Medical University, 9 West Sec. Lvshun South Road, Dalian, Liaoning Province 116044, China (Y. Zhang and H. Liu).
E-mail addresses: zoulijuan1963@sina.com (L. Zou), zhangyingqiu.no.1@163.com (Y. Zhang), liuhan@dmu.edu.cn (H. Liu).
[1] These authors contributed equally.

https://doi.org/10.1016/j.jare.2022.01.015
2090-1232/© 2022 The Authors. Published by Elsevier B.V. on behalf of Cairo University.
This is an open access article under the CC BY-NC-ND license (http://creativecommons.org/licenses/by-nc-nd/4.0/).

Lung adenocarcinoma
Endocytosis
DUB

molecule inhibitor. The combined efficacy of melatonin and USP8 suppression was also evaluated using xenograft animal models.

Results: Bioinformatic analysis revealed increased expression of the MT_1 receptor in lung adenocarcinoma tissues. Melatonin treatment leads to the downregulation of the MT_1 receptor in lung adenocarcinoma cells, which is attributed to receptor endocytosis and lysosomal degradation via the canonical *endo*-lysosomal route. USP8 negatively regulates the endocytic degradation of the MT_1 receptor incurred by melatonin exposure and thus protects lung adenocarcinoma cell growth. USP8 suppression by knockdown or pharmacological inhibition effectively deters cancer cell proliferation and sensitizes lung adenocarcinoma cells to melatonin *in vitro*. Furthermore, USP8 silencing significantly potentiates the anticancer effects of melatonin in xenograft tumor models.

Conclusion: The MT_1 receptor responds to melatonin treatment and is endocytosed for lysosomal degradation that is counteracted by USP8. The inhibition of USP8 demonstrates tumor-suppressive effects and thus can be exploited as potential therapeutic strategy either as monotherapy or combined therapy with melatonin.

© 2022 The Authors. Published by Elsevier B.V. on behalf of Cairo University. This is an open access article under the CC BY-NC-ND license (http://creativecommons.org/licenses/by-nc-nd/4.0/).

Introduction

Melatonin (N-acetyl-5-methoxytryptamine), an indoleamine neurohormone generated primarily by the pineal gland, has been revealed to participate in a diverse range of physiological processes [1]. In addition to its essential roles in regulating circadian rhythms, melatonin demonstrates anti-inflammatory and antioxidative characteristics linking it to additional beneficial roles such as cardiovascular protective and immunomodulatory functions [2–4]. Furthermore, it is worth noting that accumulating evidence from diverse experimental settings infers the oncostatic activities of melatonin towards a variety of malignancies, including lung, prostate, breast, renal and colorectal cancers [5].

Lung cancer has presented a formidable threat to human health, with both highest incidence and mortality among human neoplasms recorded globally [6]. Non-small cell lung cancer (NSCLC) is the principal subtype of human lung cancer, comprising about 80–85% of all cases. Histologically, NSCLC can be divided into 3 categories, i.e. lung adenocarcinoma (LUAD), squamous carcinoma (LUSC), and large cell carcinoma (LCC), with the former two recognized as the most frequently diagnosed subtypes (LUAD and LUSC) of human lung cancer. Importantly, the anticancer effects of melatonin towards NSCLC have been well established, which include the suppression of tumor cell proliferation, invasion and metastasis, as well as the induction of apoptosis, immunomodulation and synergy with chemo- and radio-therapies [7].

The human genome encodes two G-protein-coupled receptors that act as melatonin receptors (*MTNR1A* and *MTNR1B* for MT_1 and MT_2, respectively). Although the oncostatic activities of melatonin against a wide array of cancer types have been reported, the involvement of both MT_1 and MT_2 receptors in the cancer-suppressive functions of melatonin has so far remained less understood [5,8]. Intriguingly, the melatonin MT_1 and MT_2 receptors were shown to undergo melatonin-triggered internalization that was associated with physiological and pathological implications [9–11]. However, the dynamic regulation of MT_1 and MT_2 receptor endocytosis and the potential contribution to the anticancer effects of melatonin remain underinvestigated until now.

The current study reports the dynamic regulation of melatonin-induced MT_1 receptor endocytosis in lung adenocarcinoma cells. The ubiquitin-specific protease 8 (USP8) counteracts the endocytic degradation of MT_1 receptor incurred by melatonin treatment. In lung adenocarcinoma, USP8 depletion renders A549 and H358 cells more susceptible to melatonin-mediated inhibition, while pharmacological USP8 inhibition significantly enhances the tumor-suppressive effects of melatonin. Collectively, our observations uncover novel aspects of the endocytic regulation of the melatonin-MT_1 receptor signaling axis and hold potential for future investigation of the oncostatic efficacy of melatonin.

Materials and methods

Cell culture

All cell lines used were purchased from the American Type Culture Collection (ATCC, Manassas, USA). HEK293T cells were grown in DMEM (Dulbecco's Modified Eagle's Medium) media, and non-small cell lung cancer A549 and H358 cells were maintained in RPMI-1640 media. Culture media were supplemented with 10% of fetal bovine serum (ExCell Bio, Shanghai, China) and 1% penicillin/streptomycin (Thermo-Fisher Scientific, Waltham, USA). The stable knockdown cell lines were cultured in media containing 2 μg/ml of puromycin to maintain positive selection. Cells were kept in a humidified atmosphere at 37 °C with 5% CO_2 enabled within the cell culture incubator (3111, Thermo, Waltham, USA). Cell culture plastic wares were obtained from Guangzhou Jet Bio-Filtration Co., Ltd (Guangzhou, China).

Antibodies and other reagents

Mouse anti-MT_1 antibody (sc-390328, 1:1,000) was purchased from Santa Cruz Biotechnology (Dallas, USA). Rabbit anti-MT_1 antibody (D160637, 1:1,000) was obtained from Sangon Biotech (Shanghai, China). Mouse anti-USP8 (67321–1-Ig, 1:20,000) and anti-GAPDH (60004-1-Ig, 1:10,000) antibodies were purchased from Proteintech (Wuhan, China). Mouse anti-Tubulin antibody (T5168, 1:100,000) was purchased from Sigma (Darmstadt, Germany). Mouse anti-LAMP2 antibody (ab25631, 1:50) was obtained from Abcam (Cambridge, UK). Mouse anti-Ki-67 (610969, 1:400) and anti-EEA1 (610456, 1:500) antibodies were purchased from BD Medical Technology (Franklin Lakes, USA). Secondary infrared-labeled goat anti-mouse (926–68070, 1:15,000) and anti-rabbit (926–32211, 1:15,000) antibodies for immunoblotting were obtained from LICOR (Lincoln, USA). Alexa Fluor® 488- and 594-labeled secondary antibodies for immunofluorescence (A11001 and A11005, 1:1,000) were purchased from Invitrogen (Carlsbad, USA). Melatonin was obtained from Dalian Meilun Biotechnology Co., Ltd (Dalian, China). The GFP-MT_1 construct has been previously described, which is a generous gift from Prof. Nai-ming Zhou (Zhejiang University, China) [11]. The USP8 inhibitor was purchased from MedChem Express (Shanghai, China). Puromycin was purchased from Beijing Solarbio Science & Technology Co., Ltd (Beijing, China). Unless specified, all chemicals were purchased from Sigma (Darmstadt, Germany).

Immunoblotting

Immunoblotting assays were conducted as previously described [12]. In brief, cell lysates were acquired using "RIPA" buffer (1% Tri-

ton X-100, 10 mM Tris-HCl pH 7.5, 150 mM NaCl, 1% sodium deoxycholate, 0.1% SDS) supplemented with Na_3VO_4 (2 mM) and PMSF (1 mM). Protein concentrations were determined using BCA protein assays (Takara, Beijing, China). Equal amounts of lysates (30–50 μg) were loaded and resolved by 8% SDS-PAGE gels. Protein samples were then transferred to nitrocellulose blots (Merck Millipore, Darmstadt, Germany). Samples were subsequently blocked in 4% of fat free milk in phosphate-buffered saline (PBS) for an hour before incubated with primary antibodies at 4 °C for 4 h. Next day, membranes were washed with PBS/T (PBS with 0.1% of Tween 20) twice and then incubated with secondary antibodies for an hour, followed by two washes with PBS/T and once with PBS. Finally, blots were scanned on an infrared imaging platform (LI-COR Odyssey, Lincoln, USA) and acquired images were further analyzed using the Image Studio Programme (Version 4.0). Protein band intensities were measured with background subtraction and normalized to corresponding loading control (GAPDH) before plotted. Each experiment was repeated three times with biological replicates.

Immunofluorescence

Cells were grown on coverslips placed in 3.5-cm culture plates. Previous immunofluorescence procedures were followed [13]. After indicated treatment, cells were washed with PBS prior to fixation with 4% paraformaldehyde. After permeabilization with 0.2% of Triton X-100 in PBS, cells were treated with 2% of bovine serum albumin (BSA) in PBS at room temperature for an hour. Then samples were incubated with specific primary antibody for an hour at room temperature, followed by secondary antibody for 30 min. Finally, samples were washed in PBS and distilled water, and then coverslips were mounted onto glass slide with Mowiol (Sigma). The experiment was conducted with three biological repeats. Immunofluorescence staining was captured using a Leica fluorescence microscope (SP8, Wetzlar, Germany).

Colony formation assay

Cultured A549 (at a seeding density of 1, 000 cells per well) and H358 (at a seeding density of 4, 000 cells per well) cells were plated into 6-well plates that were maintained in the cell culture incubator. Cells were treated with 1 mM of melatonin and media were changed every two days. After two weeks, colonies were methanol fixed and stained in 0.1% of crystal violet. Images were acquired on a Bio-Rad ChemiDoc XRS + platform (Hercules, USA) and finally analyzed with the ImageJ programme. The experiments were carried out with three biological replicates.

MTT assay

Lung adenocarcinoma A549 and H358 cells were seeded into 96-well plates at a seeding density of 4, 000 cells per well and incubated overnight. The following day, cells were treated with 1 mM of melatonin for 24 h, before adding MTT (3-(4, 5-dimethylthiazol-2-yl)-2, 5-diphenyltetrazolium bromide) into each well and subsequent incubation for 3 h. Then 150 μl of DMSO were added into each well and absorbance (570 and 630 nm) was recorded using a benchtop spectrometer (Perkin Elmer, Enspire2300, Waltham, USA). The experiment was repeated with three biological replicates.

Stable cell lines

Cultured HEK293T cells were transfected with shRNA-expressing pLKO.1 plasmids (empty vector control or each of two shRNAs targeting USP2, USP8, AMSH, and AMSH-LP), along with packaging plasmids (three-plasmid system) as per the manufacturer's instructions (Sigma). Lentiviruses were collected after 48 h and used to infect A549 and H358 cells. Positive expression cells were selected using treatment with 2 μg/ml of puromycin and knockdown efficiency was confirmed with standard semi-quantitative RT-PCR assays. USP8 knockdown efficiency was further evaluated by Western blotting. DUB-specific shRNA sequences were described previously [14].

Xenograft mouse model

Animal experiments were conducted in accordance with the 1996 National Institute of Health Guide for the Care and Use of Laboratory Animals. Experimental protocols were approved by the Institutional Animal Care and Use Committee at Dalian Medical University. Six-week-old female nude mice (Balb/c background, Charles River, Beijing, China) were randomly distributed into two groups (10 mice/group). A549-pLKO.1 (vector control) and A549-USP8-sh1 (USP8 shRNA1-expressing) stable cells (2 million/mouse) were subcutaneously implanted into mice from two groups separately. Mice were maintained in a pathogen-free condition during the entire experiment and tumor volume was measured with a vernier caliper every 2 days during the whole 37-day period before reaching size limitation. After one week, mice from each group were further divided into two groups (5 mice/group), which were administered with melatonin (25 mg/kg) or DMSO as vehicle control by intraperitoneal injection at 7 pm every day for 30 days [15]. Tumor volume was estimated according to the formula: tumor volume (mm^3) = (length) × $(width)^2 \times 0.5$.

Immunohistochemistry

Xenograft tumors were fixed in 4% paraformaldehyde overnight before paraffin-embedding. Tissue sections (4 μm) were prepared and dried at 56 °C for 4 h before deparaffinized and rehydrated with graded alcohol. Following incubation with blocking solution using the IHC assay kit (ZSGB-Bio, Beijing, China), tissue sections were treated with primary antibody for overnight at 4 °C. Next day, tissue sections were stained using the IHC assay kit as per the manufacturer's instructions. Samples were visualized and images were acquired using a Leica microscope (DMI4000B, Wetzlar, Germany). Randomly chosen fields from each mounted section were analyzed and quantitated with the Image-Pro Plus programme (version 6.0).

Statistics

Experiments were repeated for at least three times with biological replicates. Quantification data were analyzed by one-way ANOVA or Student's *t*-test using GraphPad Prism (version 7) for multiple group or paired sample comparisons, respectively. Individual data points were presented in quantification plots, with $p < 0.05$ considered as statistically significant.

Results

Melatonin-triggered MT_1 endocytosis is associated with receptor degradation

Accumulating RNA sequencing data from cancer consortium projects have tremendously enhanced our understanding about the transcriptomic characteristics of various types of cancer [16]. Using the web-based GEPIA (Gene Expression Profiling Interactive Analysis) platform, we analyzed the RNA expression levels of both melatonin receptors in non-small cell lung cancer (LUAD and LUSC)

and non-cancerous samples [17]. As demonstrated in Fig. 1A and B, in general, the expression of MT_1 receptor appears higher than MT_2 in both LUAD and LUSC specimens, with higher average levels of MT_1 observed in LUAD than in LUSC. Therefore, we decided to focus on the MT_1 receptor in LUAD for subsequent investigation.

We treated lung adenocarcinoma A549 and H358 cells with pharmacological dose of melatonin before performing immunoblotting analyses [18]. Results from immunoblotting assays show that melatonin exposure led to a gradual reduction in the protein levels of MT_1 receptor over a 12 h period in both cell lines (Fig. 1C and D). Such quick responses of MT_1 protein abundance to melatonin treatment within hours indicated that changes likely occurred at the protein level rather than at the mRNA level of MT_1 expression [19]. To acquire an optimal visualization of MT_1 receptor localization in the cell, we exogenously expressed GFP-tagged MT_1 receptor in HeLa cells and performed fluorescence investigation following melatonin treatment. In untreated cells, MT_1 receptor was observed on both the plasma membrane and within the cell in the cytoplasm, while melatonin addition markedly enhanced MT_1 internalization leading to its significantly reduced distribution to the surface (Fig. 1E). In light of the evidence that cell surface receptors are frequently turned over by endocytic degradation through lysosomes, we posited that internalized MT_1 receptor was possibly routed through endosome system for lysosomal degradation [20]. Indeed, when the cells were incubated in chloroquine to impede lysosomal function, we observed enhanced GFP fluorescence signal within the cell following melatonin incubation, intimating accumulated MT_1 receptors that were unable to go through lysosomal destruction (Fig. 1F) [21].

Internalized MT_1 receptor is sorted through the canonical endo-lysosomal route

To gain more mechanistic insights into the intracellular trafficking of internalized MT_1 receptor, we conducted immunofluorescence and confocal microscopy experiments to investigate the colocalization of endocytosed MT_1 receptor with established markers of early endosomes (Early endosome antigen 1, EEA1) and late endosomes/lysosomes (Lysosome-associated membrane glycoprotein 2, LAMP2), respectively [21]. As described in Fig. 2A and B, in untreated cells, GFP-tagged MT_1 receptor appeared to be largely separate from both EEA1 and LAMP2 staining, illustrating only sparse colocalization of the MT_1 receptor with endosomal structures under steady state conditions that likely represented constitutive receptor turnover by endocytosis. However, following 6 h of melatonin treatment, internalized MT_1 receptor showed widespread colocalization with the early endosomal marker EEA1, as well as evident colocalization with the late endosomal marker LAMP2 (Fig. 2A and B). After 24 h of melatonin exposure, the colocalization of the MT_1 receptor with EEA1 was dramatically attenuated (Fig. 2A), whilst its association with the late endosomes and lysosomes persisted as revealed by LAMP2 staining (Fig. 2B), suggesting that the majority of MT_1 receptor was already trafficked through early endosomes to reach late endosomes or lysosomes.

Furthermore, we treated cells with chloroquine to block lysosomal function aiming to investigate the potential degradation of internalized MT_1 receptor following melatonin incubation. As illustrated in Fig. 2C, over a 12 h incubation period, inhibition of lysosomal degradation imposed by chloroquine treatment led to a significant accumulation of the MT_1 receptor on structures marked with LAMP2 staining, indicating a buildup of unprocessed MT_1 receptor that was sorted to the lysosome incurred by melatonin treatment. Hence, these observations collectively show the dynamic transportation of the MT_1 receptor along the canonical endosomal track for destruction in the lysosome following melatonin treatment, which also complies with the well established models of endocytic degradation of cell surface receptors [22–24].

USP8 obstructs melatonin-induced endocytic degradation of the MT_1 receptor

The endocytic degradation of a slew of cell surface receptors has been demonstrated as a dynamically regulated process, in which several deubiquitylases are frequently observed to regulate the dynamics of receptor degradation predominantly via catalyzing the removal of ubiquitin moieties off receptors or receptor-associated proteins [25]. Among the deubiquitylase superfamily that contains close to 100 proteins, 4 members (USP2, USP8, AMSH, and AMSHLP) have been shown to localize to the endosome/lysosome system and experimentally revealed to regulate diverse receptor endocytosis procedures [14,26,27]. Therefore, we speculated that certain endosome-associated deubiquitylase might exert function in the regulation of melatonin-incurred endocytic degradation of the MT_1 receptor. To test this hypothesis, we knocked down the expression of each of the four endosome-associated deubiquitylases using an shRNA-based approach (two separate shRNAs per target). While comparing the levels of the MT_1 receptor in these 8 shRNA-expressing stable cell lines to that in vector control A549 cells under steady state conditions, we found that the MT_1 receptor expression was significantly compromised in both USP8 shRNA-expressing A549 cells (Fig. 3A).

We next sought to tease out how USP8 silencing led to reduced MT_1 receptor expression under steady state conditions and thus measured the mRNA levels of the MT_1 receptor in control and USP8 shRNA-expressing A549 cells by performing semi-quantitative polymerase chain reaction assays. Since the MT_1 receptor mRNA expression was not significantly affected by USP8 knockdown (Fig. 3B), we reasoned that the reduction in MT_1 receptor occurred post-transcriptionally. Therefore, we carried out cycloheximide chase experiments that measure protein stability through blocking polypeptide synthesis, in order to assess the turnover rates of the MT_1 receptor in control and USP8-depleted cells [28]. As shown in Fig. 3C, in USP8 shRNA-expressing A549 cells, the degradation of MT_1 receptor turned out to be accelerated compared to it was in control A549 cells, suggesting that the enhanced turnover imposed by USP8 depletion was likely the main reason for decreased levels of MT_1 receptor. To examine the influence of USP8 knockdown on melatonin-induced downregulation of the MT_1 receptor, we performed further immunoblotting experiments using these established stable cell lines. As demonstrated in Fig. 3D and E, USP8 silencing led to further MT_1 receptor downregulation incurred by melatonin treatment. Therefore, these findings collectively indicate that USP8 safeguards the MT_1 receptor expression levels under both steady state and melatonin treatment conditions, and accordingly shRNA-mediated USP8 silencing results in attenuated MT_1 receptor expression through enhancing its degradation.

USP8 depletion sensitizes lung adenocarcinoma cells to melatonin

Although the anticancer effects of melatonin against lung cancer have become well-documented, the exact roles of the MT_1 receptor in the oncostatic activities of melatonin appear understudied. Given that the melatonin-MT_1 receptor axis has been linked to multiple downstream signaling molecules including G proteins and MAP kinases that are recognized as key factors during tumorigenesis, it is of great importance to understand the roles that the MT_1 receptor and its endocytosis play in cancer cells treated with melatonin. In doing this, we performed cell proliferation and colony formation assays using lung adenocarcinoma cells with or without USP8 knockdown. Considering the evidence that USP8

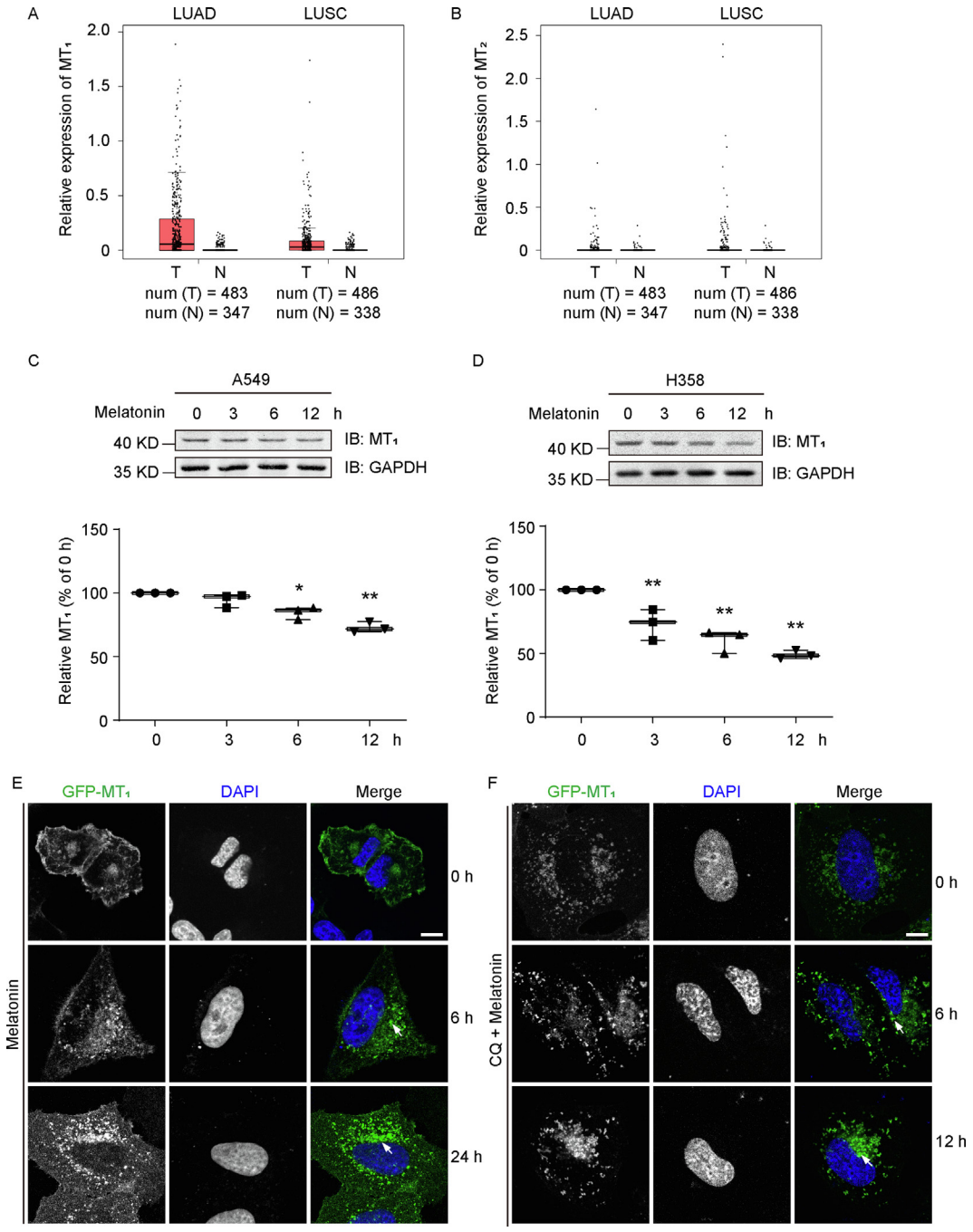

Fig. 1. Melatonin induces MT_1 downregulation and internalization. **A** and **B** The mRNA levels of MT_1 (A) and MT_2 (B) in tumor and paired normal tissues from patients of lung adenocarcinoma (LUAD) and lung squamous carcinoma (LUSC) were analyzed using TCGA data retrieved from the GEPIA website (http://gepia.cancer-pku.cn/). C and **D** A549 and H358 cells as indicated were treated with 1 mM of melatonin for 0, 3, 6, and 12 h before cell lysis and immunoblotting analysis using indicated antibodies. GAPDH was detected to show equal loading. The graphs below show the relative quantification of MT_1 levels. Individual data points were shown at corresponding times (n = 3). Statistical difference was evaluated by performing one-way ANOVA, with * and ** showing $p < 0.05$ and $p < 0.01$, respectively. **E** HeLa cells were transfected with the GFP-MT_1-expressing construct. Cells were treated with melatonin (1 mM) for indicated times and then processed for immunofluorescence analysis. DAPI stains the nucleus. Images show representative confocal sections. Scale bar = 10 μm. **F** HeLa cells transfected with the GFP-MT_1 construct were pretreated with chloroquine (100 μM) for 30 min before melatonin (1 mM) incubation for indicated times. Samples were analyzed by immunofluorescence and confocal microscopy. DAPI staining shows the nucleus. Images show representative confocal sections. Scale bar = 10 μm.

also regulates the endocytic degradation of the epidermal growth factor receptor (EGFR) that acts as a pivotal oncogenic driver in lung adenomas, we selected A549 and H358 cell lines that contain activating mutations in KRAS downstream of EGFR and thus can bypass the inhibition on EGFR imposed by USP8 silencing in these assays [29].

The results from MTT assays measuring cell growth over a 24 h period showed that shRNA-mediated USP8 depletion rendered both A549 and H358 cells reduced cell proliferation as compared to control vector-containing cells (Fig. 4A). Consistent with previous findings, melatonin treatment effectively decreased cell propagation in both A549 and H358 lung adenocarcinoma cells, while the extent of growth inhibition imposed by melatonin over a 24 h duration was comparable in A549 and H358 cells with USP8 silencing as revealed by MTT assays (Fig. 4B). However, data from long-term colony formation assays revealed even stronger

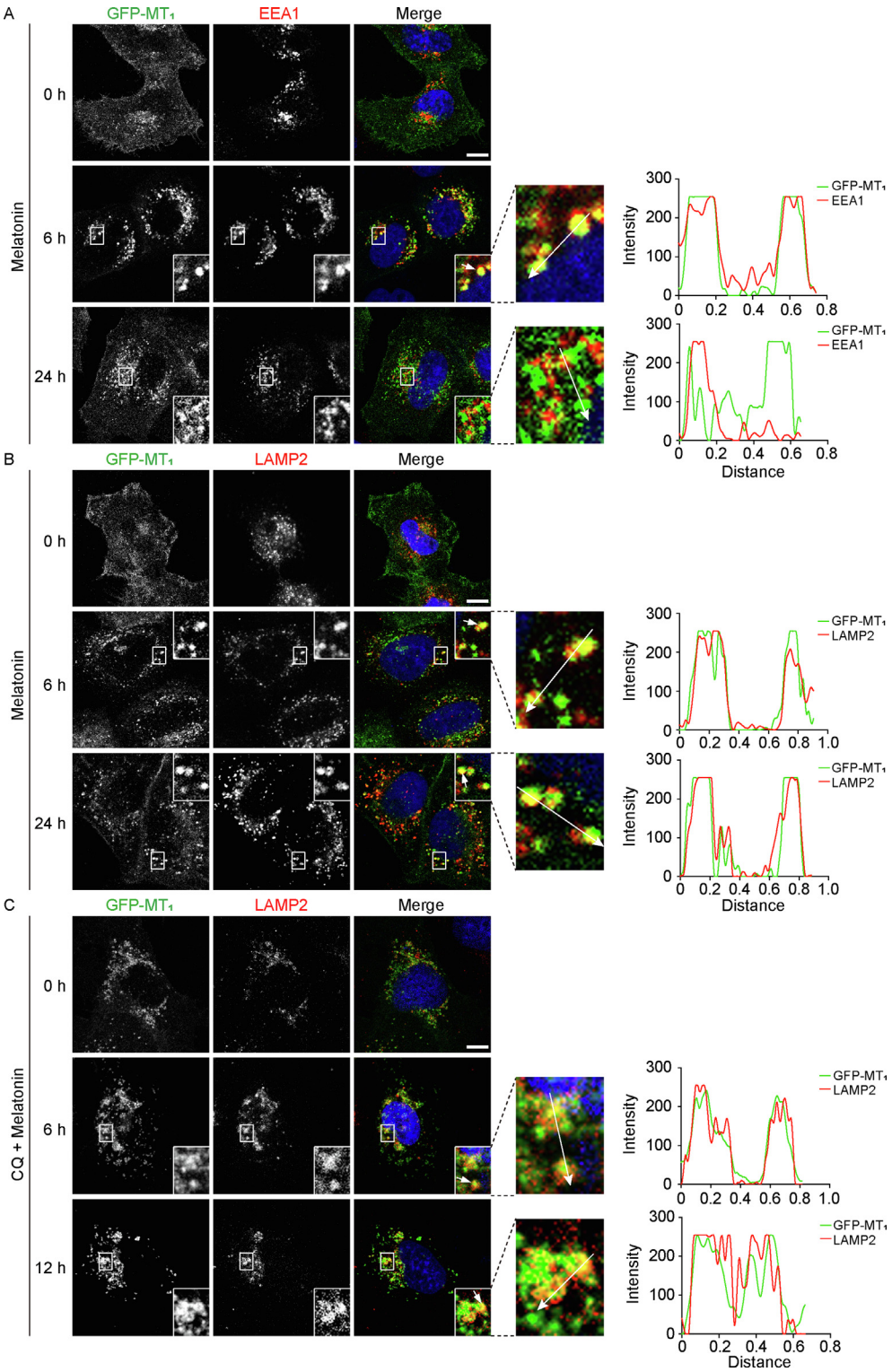

Fig. 2. Endocytosed MT_1 is sorted through the endo-lysosomal pathway. A and B HeLa cells transfected with the GFP-MT_1 construct were treated with melatonin (1 mM) for indicated times. The colocalization of GFP-tagged MT_1 with endogenous EEA1 (A) and LAMP2 (B) was inspected by immunofluorescence and confocal microscopy. Nucleus was stained with DAPI. Representative confocal sections are shown with magnified insets to illustrate colocalization. Graphs on the right show the quantification of fluorescence intensities for GFP-MT_1 (green) and EEA1 or LAMP2 (red). Scale bar = 10 μm. C HeLa cells transiently expressing GFP-MT_1 were pretreated with chloroquine (CQ) for 30 min prior to melatonin exposure for 0, 6, and 12 h. Samples were then analyzed by confocal microscopy. Micrographs show representative confocal sections, with magnified insets demonstrating the colocalization of GFP-MT_1 with LAMP2. Graphs on the right demonstrate quantification. Scale bar = 10 μm.

influence of USP8 knockdown on the growth of A549 and H358 lung adenocarcinoma cells, suggesting an accumulative effect of USP8 silencing in these cells (Fig. 4C). Importantly, the results from colony formation assays demonstrated even stronger inhibitory effects of melatonin treatment on both A549 and H358 cells with stable USP8 knockdown, suggesting that USP8 depletion sensitized

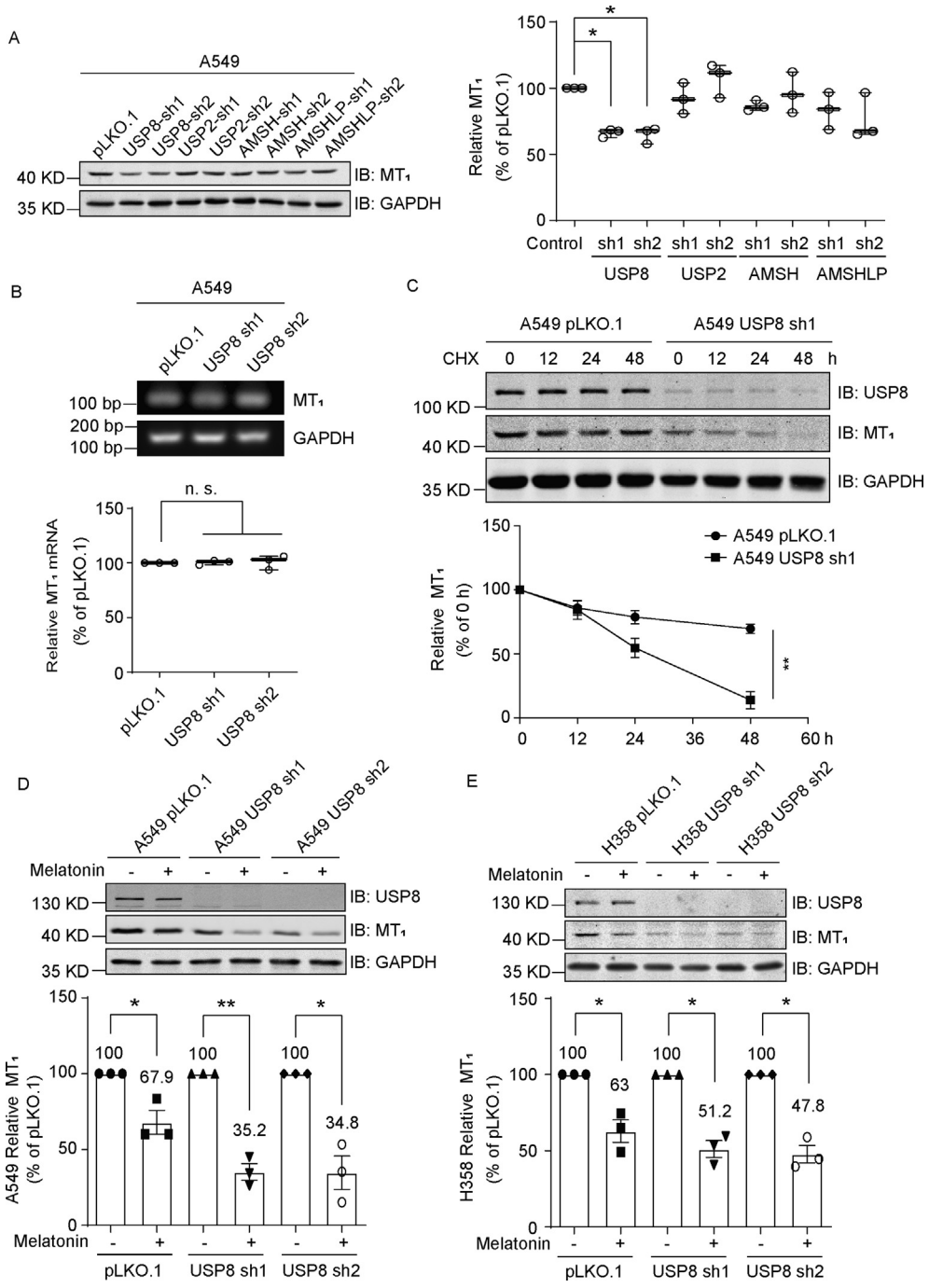

Fig. 3. USP8 silencing accelerates the turnover of MT_1. A A549 cells with stable knockdown of USP8, USP2, AMSH and AMSHLP (two shRNAs for each target and pLKO.1 vector as control) were lysed and subjected to immunoblotting analysis with anti-MT_1 antibody. GAPDH was detected to show equal loading. Graph on the right shows quantification data of MT_1 levels from 3 biological repeats. B A549-pLKO.1 and USP8 knockdown cells were harvested to extract total RNA. Relative mRNA levels of MT_1 were assessed by RT-PCR assays with specific primers. GAPDH mRNA levels were detected to illustrate equal loading. Graph below demonstrates quantification data of the relative mRNA amounts of MT_1 (n. s., not significant). C A549-pLKO.1 and USP8 knockdown cells were treated with cycloheximide (100 μg/ml) for indicated times and lysed. Samples were analyzed by immunoblotting with anti-USP8 and anti-MT_1 antibodies. GAPDH blot indicates equal loading. The graph below shows quantification data of relative MT_1 levels. D and E A549-pLKO.1 and USP8 knockdown cells (D) as well as H358-pLKO.1 and USP8 knockdown cells (E) were treated with melatonin at 1 mM for 24 h. Cell lysates were analyzed by immunoblotting with anti-USP8 and anti-MT_1 antibodies. GAPDH was probed to confirm equal loading. Column charts below show the quantification of relative MT_1 levels with mean values labeled on top. Individual data points were indicated for quantification plots, with * and ** indicating $p < 0.05$ and $p < 0.01$, respectively.

lung adenocarcinoma cells to melatonin exposure (Fig. 4D and E). Taken together, these observations hence indicate the potential tumor-supportive role of USP8 in lung adenocarcinoma is likely linked to its impact on the endocytic degradation of the melatonin receptor MT_1.

USP8 small molecule inhibitor potentiates the tumor-suppressive effects of melatonin

Since ubiquitin-specific proteases are deemed as actionable targets for pharmacological interference, we next sought to test the

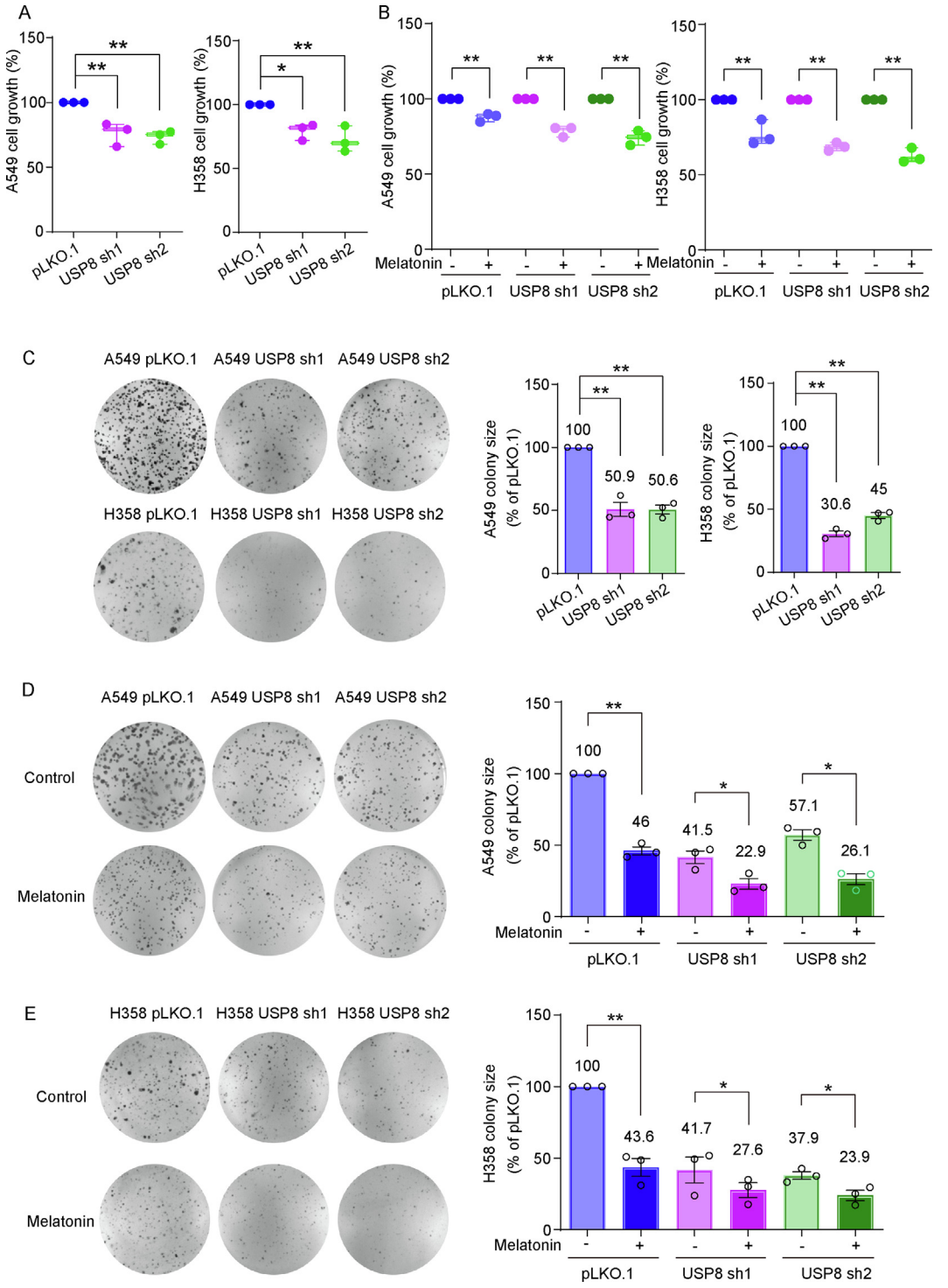

Fig. 4. USP8 silencing inhibits the propagation of lung adenocarcinoma cells and potentiates melatonin-imposed growth suppression. **A** Cell proliferation of A549 and H358 cells stably transfected with pLKO.1 and USP8 shRNA constructs were evaluated by MTT assays. Graphs show data from 3 independent experiments. **B** A549 and H358 cells stably transfected with pLKO.1 and USP8 shRNA constructs were treated with 1 mM of melatonin for 24 h. Cell viability was assessed with MTT assays. Graphs show data from 3 independent experiments. **C** Colony formation assays with A549 and H358 control and USP8 knockdown cell lines. Column charts on the right show the relative sizes of colonies formed in each group, with mean values labeled on top. **D** and **E** Colony formation assays using A549 (D) and H358 (E) control and USP8 knockdown cells with or without melatonin treatment at 1 mM. Column charts on the right show the relative sizes of colonies formed in each group, with mean values labeled on top. Individual data points were indicated for quantification plots, with * and ** showing $p < 0.05$ and $p < 0.01$, respectively.

influence of USP8 chemical inhibitor on the *in vitro* growth of lung adenocarcinoma cells in the presence of melatonin treatment [30,31]. Using synthesized 9-[(phenylmethoxy)imino]-9*H*-indeno[1,2-b]pyrazine-2,3-dicarbonitrile) that is an analogue of 9-oxo-9*H*-indeno[1,2-b]pyrazine-2,3-dicarbonitrile and reported by Colombo *et al.* to have an IC50 of 0.71 μM against USP8, we carried out MTT and colony formation assays with or without melatonin addition [32]. Again we used A549 cells that endogenously express constitutively active KRAS mutants, in order to rule out potential effects attributed by the influence on EGFR dynamics imposed by

USP8 inhibition. The results from MTT assays showed that this USP8 inhibitor exerted a dose-dependent inhibitory effect on the proliferation of A549 cells, which were consistent with data obtained from shRNA-mediated USP8 depletion experiments (Fig. 5A).

Furthermore, data from subsequent MTT assays to measure cell proliferation over a 24 h incubation period under the treatment with melatonin (1 mM), the USP8 inhibitor (0.6 μM), or the combination revealed analogous extent of growth inhibition (Fig. 5B). However, with colony formation assays that recorded long-term cell propagation, treatment with melatonin and the USP8 inhibitor resulted in further decreased cell growth compared to the effects observed with MTT assays, while the combined treatment with melatonin and USP8 inhibitor led to a significantly enhanced defect in the colony formation of A549 cells than single treatment groups (Fig. 5C and D). Therefore, these observations indicate that the pharmacological inhibition of USP8 deubiquitylase could not only elicit a tumor-suppressive effect towards lung adenocarcinoma, but also potentiate the anticancer effects of melatonin.

USP8 silencing enhances the anticancer effect of melatonin in xenograft animal model

Having demonstrated the suppressive roles of USP8 inhibition in lung adenocarcinoma cell growth *in vitro*, we next turned to investigate the impact of USP8 suppression on the *in vivo* tumor xenograft formation of lung A549 cells in nude mice. In doing this, A549 cells stably transfected with control and USP8 shRNA-expressing vectors were subcutaneously implanted into athymic nude mice with Balb/c background. Xenograft tumors were recorded and mice were randomized into four groups to receive melatonin or control vehicle: A549 pLKO.1 administered with DMSO or melatonin and A549 pLKO.1-USP8-sh1 administered with DMSO or melatonin. As shown in Fig. 6A and B, USP8 depletion rendered A549 cells attenuated xenograft tumor formation in nude mice, while melatonin treatment displayed inhibitory effects on the *in vivo* growth of A549 cells with or without USP8 knockdown. As a result, xenograft tumors from the A549 pLKO.1-USP8-sh1 group received melatonin treatment were recorded with the smallest size on average and hence were most significantly suppressed as compared to the control group (Fig. 6C). Interestingly, Western blotting analyses of xenograft samples revealed an upregulation of USP8 expression in melatonin-treated A549 group, suggesting a potential positive regulation of USP8 abundance by melatonin treatment (Fig. 6D and E). Consistent with our *in vitro* observations, the expression levels of the melatonin MT_1 receptor in A549 xenograft tumors were down regulated by melatonin treatment and USP8 knockdown, with the lowest levels on average observed in the xenograft samples from the A549 pLKO.1-USP8-sh1 group treated with melatonin (Fig. 6D and E). Congruently, immunohistochemistry analyses of xenograft tumor samples further confirmed the inhibitory effects of USP8 depletion and melatonin treatment on MT_1 expression and tumorigenesis, which were revealed by the staining of MT_1 and the proliferation marker Ki-67, respectively (Fig. 6F and G). Taken together, our data from *in vivo* xenograft animal model study corroborate the tumor-protective implications of USP8 and intimate it as a potential therapeutic target in the treatment of lung adenocarcinoma either as monotherapy or in combination modalities such as with melatonin.

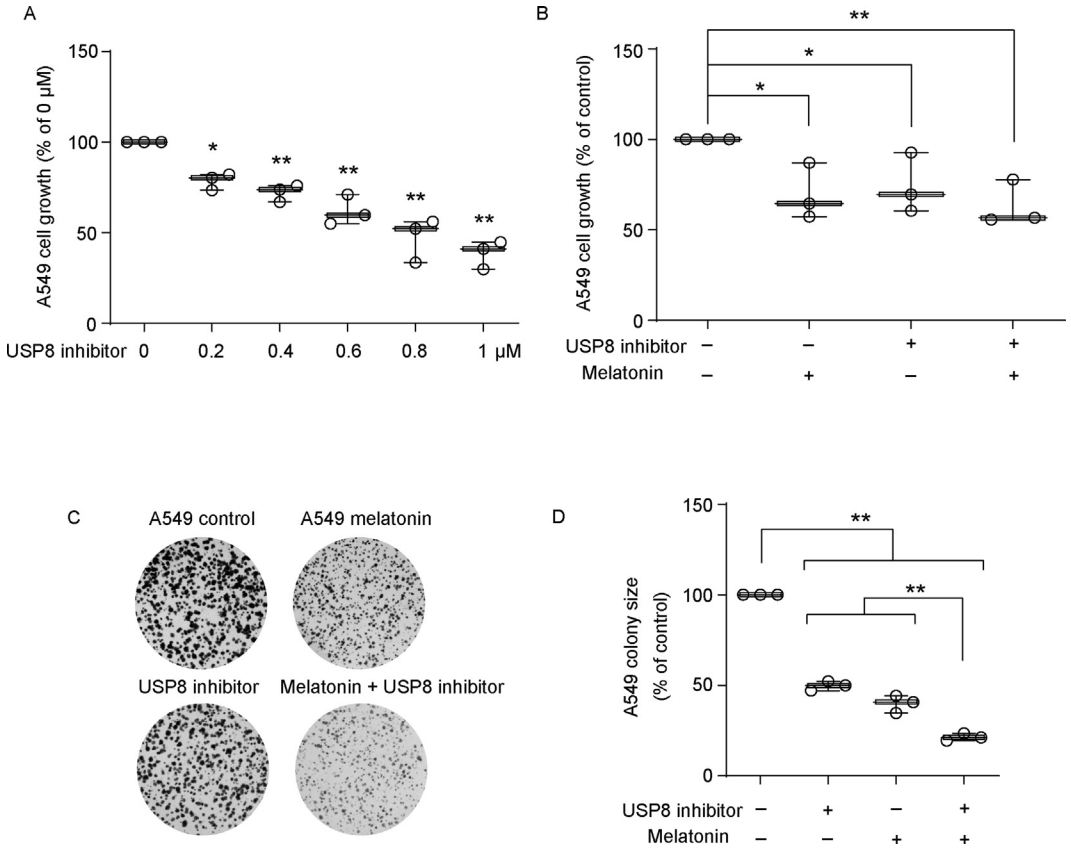

Fig. 5. Pharmacological USP8 inhibition sensitizes lung adenocarcinoma cells to melatonin. **A** A549 cells were treated with the USP8 inhibitor at indicated concentrations for 24 h. Cell viability was examined with MTT assays. Graph shows data from 3 independent experiments. **B** A549 cells were treated with the USP8 inhibitor (0.6 μM), melatonin (1 mM), or the combination as indicated for 24 h. Cell viability was evaluated with MTT assays. Graph shows data from 3 independent experiments. **C** Colony formation assays of A549 cells with the treatment of the USP8 inhibitor (0.6 μM), melatonin (1 mM), or the combination as indicated. **D** Graph shows the quantification of C (n = 3).Individual data points were shown for quantification plots, with * and ** showing $p < 0.05$ and $p < 0.01$ relative to untreated controls as indicated, respectively.

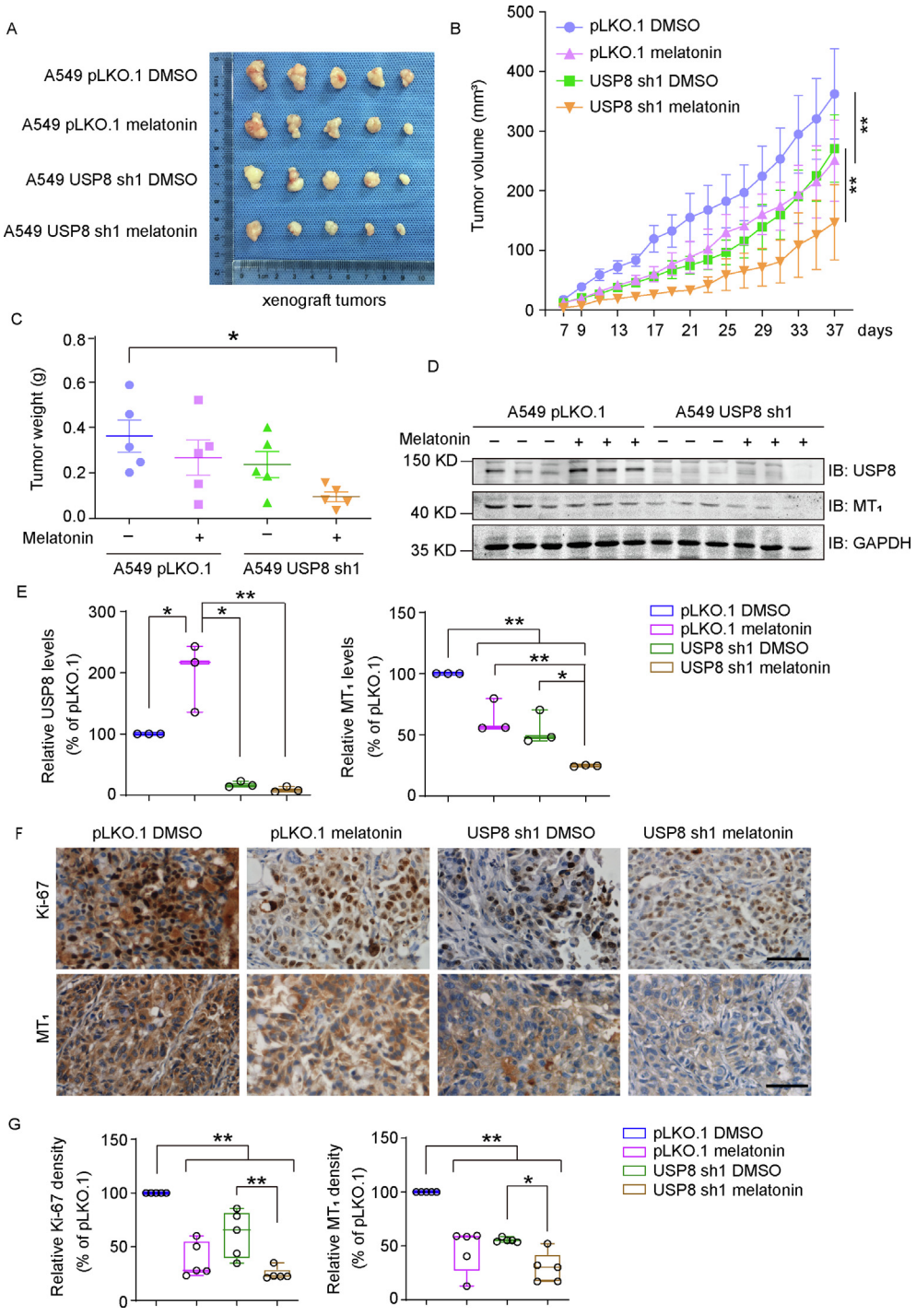

Fig. 6. Depletion of USP8 potentiates the inhibitory effects of melatonin on xenograft tumor growth. **A** A549 pLKO.1 and USP8 knockdown cells were inoculated into Balb/c female nude mice to generate tumor xenografts. Mice were randomly divided into groups to receive melatonin or vehicle (DMSO) treatment via intraperitoneal injection. Image shows the resected xenograft tumors. **B** The tumor volumes from four experimental groups were measured and plotted. DMSO and melatonin treatment groups were compared as indicated to examine statistical difference using *t*-test (n = 5). ** shows $p < 0.01$. **C** Weights of resected tumors were measured and plotted. *T*-test was performed to compare difference (n = 5). **D** The resected tumors were lysed to prepare protein samples that were analyzed by immunoblotting with anti-USP8, anti-MT_1, and anti-GAPDH antibodies. **E** Quantification data from D show relative levels of USP8 and MT_1 in xenograft samples (n = 3). **F** Immunohistochemistry assays of xenograft tumors from each group as indicated using anti-Ki-67 and anti-MT_1 antibodies. Images show representative xenograft sections. Scale bar = 50 μm. **G** Box plots demonstrate quantification data (integral optical density) of relative intensities of Ki-67 and MT_1 from xenograft samples in F. Individual data points were indicated for quantification plots, with * and ** showing $p < 0.05$ and $p < 0.01$, respectively.

Discussion

Lung cancer has remained a leading threat to human health and is recorded with steadily high morbidity and mortality globally [33]. Therefore, this challenge calls for continuous investigation into this malignancy and the development of additional efficient therapeutic strategies [34]. Recent advances in targeted therapy and immune therapy have tremendously improved patient outcomes. However, clinically approved therapeutic targets exemplified by EGFR, Anaplastic Lymphoma kinase

(ALK), and the PD-1/PD-L1 immune checkpoint axis are only applicable to a small proportion of lung cancer patients, and accordingly additional actionable therapeutic targets are in great request to design potential treatment modalities. The human deubiquitylases (DUBs) are a group of cysteine proteases and metalloenzymes that have been associated with a wide range of cellular activities including the dynamic regulation of cell surface receptors [35,36]. Endocytosis-associated deubiquitylases exemplified by AMSH, USP8, and USP2 have been shown to regulate the dynamic turnover of top therapeutic targets in cancer treatment such as EGFR and ErbB2/HER2 [14,29,37].

The deubiquitylase USP8, also known as ubiquitin isopeptidase Y (UBPY), belongs to the USP subfamily of human DUBs [38]. USP8 was initially identified as a growth-regulated isopeptidase and subsequently revealed to exhibit tumorigenic roles in many cancer types, such as lung cancer, cervical cancer, cholangiocarcinoma, breast cancer, and pituitary tumor [39–41]. Although demonstrating pleiotropic functions to promote tumorigenesis, the endocytic regulation of cell surface receptor dynamics has been recognized as a canonical role of USP8 [42–44]. In this study, we provide evidence that USP8 deters the melatonin-induced endocytic degradation of the MT_1 receptor, thus displaying a tumor-supportive role in lung adenocarcinoma. Although the oncostatic activities of melatonin have been well documented, the involvement and dynamic regulation of its physiological receptors MT_1 and MT_2 in lung adenocarcinoma appear to be incompletely investigated until now. Since the melatonin receptors are linked to multiple downstream signaling modules that play pivotal roles during tumorigenesis, it is of great significance to fully understand the effects of melatonin treatment. Our observations uncover the obscure aspect of the MT_1 receptor dynamics and reveal a positive regulatory role of USP8. We provide evidence that melatonin treatment triggers the internalization and endocytic sorting of the MT_1 receptor towards lysosomal degradation acting as a negative feedback mechanism to down tune the melatonin-MT_1 receptor signaling output, while the endosomal DUB USP8 antagonizes such negative modulation to spur cancer cell growth.

Conclusion

Our findings uncover the dynamic regulation of the MT_1 receptor endocytosis and hence gain novel insights into the complexity of melatonin treatment on malignant cells. Furthermore, the observations can be exploited to design targeted therapeutic strategies to enhance the efficacy of melatonin, which has been experimentally validated. With the increasing appreciation of the tumor-promoting effects of human DUBs and the susceptibility of these cysteine proteases to pharmacological interference, USP8 holds potential to serve as a leading paradigm from the DUB family proteases as a therapeutic target in cancer treatment [31,45,46].

Compliance with Ethics Requirements

Ethics statement: All procedures followed were in accordance with the 1996 National Institute of Health Guide for the Care and use of Laboratory Animals and the ethical standards approved by the Institutional Animal Care and Use Committee of Dalian Medical University.

CRediT authorship contribution statement

Qianhui Sun: Investigation, Data curation, Formal analysis. **Jinrui Zhang:** Investigation, Formal analysis. **Xiaoxi Li:** Investigation. **Guoheng Yang:** Investigation. **Shaoxuan Cheng:** Investigation. **Dong Guo:** Investigation. **Qingqing Zhang:** Investigation. **Feng Sun:** Investigation. **Feng Zhao:** Investigation. **Dian Yang:** Formal analysis. **Shanshan Wang:** Formal analysis. **Taishu Wang:** Formal analysis. **Shuyan Liu:** Formal analysis. **Lijuan Zou:** Conceptualization. **Yingqiu Zhang:** Conceptualization, Supervision. **Han Liu:** Conceptualization, Supervision, Funding acquisition, Writing – original draft, Writing – review & editing.

Declaration of Competing Interest

The authors declare that they have no known competing financial interests or personal relationships that could have appeared to influence the work reported in this paper.

Acknowledgement

The authors are grateful to Prof. Nai-ming Zhou (Zhejiang University) for generously providing the MT_1 expression construct. This work was supported by grant from the National Natural Science Foundation of China (No. 82073315 to HL). HL was also supported by LiaoNing Revitalization Talents Program (XLYC1807079) and grant from the Education Department of Liaoning Province (LZ2020001).

Appendix A. Supplementary material

Supplementary data to this article can be found online at https://doi.org/10.1016/j.jare.2022.01.015.

References

[1] Boutin JA, Audinot V, Ferry G, Delagrange P. Molecular tools to study melatonin pathways and actions. Trends Pharmacol Sci 2005;26(8):412–9.
[2] Claustrat B, Leston J. Melatonin: Physiological effects in humans. Neurochirurgie 2015;61(2-3):77–84.
[3] Tengattini S, Reiter RJ, Tan DX, Terron MP, Rodella LF, Rezzani R. Cardiovascular diseases: protective effects of melatonin. J Pineal Res 2008;44:16–25.
[4] Carrillo-Vico A, Lardone P, Álvarez-Sánchez N, Rodríguez-Rodríguez A, Guerrero J. Melatonin: buffering the immune system. Int J Mol Sci 2013;14(4):8638–83.
[5] Li Ya, Li S, Zhou Y, Meng X, Zhang J-J, Xu D-P, et al. Melatonin for the prevention and treatment of cancer. Oncotarget 2017;8(24):39896–921.
[6] Bray F, Ferlay J, Soerjomataram I, Siegel RL, Torre LA, Jemal A. Global cancer statistics 2018: GLOBOCAN estimates of incidence and mortality worldwide for 36 cancers in 185 countries. CA Cancer J Clin 2018;68(6):394–424.
[7] Ma Z, Yang Y, Fan C, Han J, Wang D, Di S, et al. Melatonin as a potential anticarcinogen for non-small-cell lung cancer. Oncotarget 2016;7(29):46768–84.
[8] Srinivasan V, Spence DW, Pandi-Perumal SR, Trakht I, Cardinali DP. Therapeutic actions of melatonin in cancer: possible mechanisms. Integrative Cancer Therapies 2008;7(3):189–203.
[9] Bondi CD, McKeon RM, Bennett JM, Ignatius PF, Brydon L, Jockers R, et al. MT1 melatonin receptor internalization underlies melatonin-induced morphologic changes in Chinese hamster ovary cells and these processes are dependent on Gi proteins, MEK 1/2 and microtubule modulation. J Pineal Res 2008;44(3):288–98.
[10] Sethi S, Adams W, Pollock J, Witt-Enderby PA. C-terminal domains within human MT1 and MT2 melatonin receptors are involved in internalization processes. J Pineal Res 2008;45(2):212–8.
[11] Hong LJ, Jiang Q, Long S, Wang H, Zhang LD, Tian Y, et al. Valproic Acid Influences MTNR1A Intracellular Trafficking and Signaling in a beta-Arrestin 2-Dependent Manner. Mol Neurobiol 2016;53:1237–46.
[12] Liu S, Wang T, Shi Y, Bai Lu, Wang S, Guo D, et al. USP42 drives nuclear speckle mRNA splicing via directing dynamic phase separation to promote tumorigenesis. Cell Death Differ 2021;28(8):2482–98.
[13] Wu Y, Zhang Y, Wang D, Zhang Y, Zhang J, Zhang Y, et al. USP29 enhances chemotherapy-induced stemness in non-small cell lung cancer via stabilizing Snail1 in response to oxidative stress. Cell Death Dis 2020;11:796.
[14] Zhang J, Liu S, Li Q, Shi Y, Wu Y, Liu F, et al. The deubiquitylase USP2 maintains ErbB2 abundance via counteracting endocytic degradation and represents a therapeutic target in ErbB2-positive breast cancer. Cell Death Differ 2020;27:2710–25.
[15] Hao J, Fan W, Li Y, Tang R, Tian C, Yang Q, et al. Melatonin synergizes BRAF-targeting agent vemurafenib in melanoma treatment by inhibiting iNOS/

hTERT signaling and cancer-stem cell traits. J Exp Clin Cancer Res : CR 2019;38:48.
[16] Hong M, Tao S, Zhang L, Diao LT, Huang X, Huang S, et al. RNA sequencing: new technologies and applications in cancer research. J Hematol Oncol 2020;13:166.
[17] Tang Z, Li C, Kang B, Gao G, Li C, Zhang Z. GEPIA: a web server for cancer and normal gene expression profiling and interactive analyses. Nucleic Acids Res 2017;45:W98–W102.
[18] Gao Y, Xiao X, Zhang C, Yu W, Guo W, Zhang Z, et al. Melatonin synergizes the chemotherapeutic effect of 5-fluorouracil in colon cancer by suppressing PI3K/AKT and NF-kappaB/iNOS signaling pathways. J Pineal Res 2017;62.
[19] Schwanhausser B, Busse D, Li N, Dittmar G, Schuchhardt J, Wolf J, et al. Global quantification of mammalian gene expression control. Nature 2011;473:337–42.
[20] Clague MJ, Liu H, Urbe S. Governance of endocytic trafficking and signaling by reversible ubiquitylation. Dev Cell 2012;23:457–67.
[21] Zhang Y, Zhang J, Liu C, Du S, Feng L, Luan X, et al. Neratinib induces ErbB2 ubiquitylation and endocytic degradation via HSP90 dissociation in breast cancer cells. CancerLett 2016;382:176–85.
[22] Mosesson Y, Mills GB, Yarden Y. Derailed endocytosis: an emerging feature of cancer. Nat Rev Cancer 2008;8(11):835–50.
[23] Goh LK, Sorkin A. Endocytosis of receptor tyrosine kinases. Cold Spring Harbor Perspect Biol 2013;5.
[24] Sigismund S, Confalonieri S, Ciliberto A, Polo S, Scita G, Di Fiore PP. Endocytosis and signaling: cell logistics shape the eukaryotic cell plan. Physiol Rev 2012;92:273–366.
[25] McCann AP, Scott CJ, Van Schaeybroeck S, Burrows JF. Deubiquitylating enzymes in receptor endocytosis and trafficking. Biochem J 2016;473:4507–25.
[26] Urbe S, Liu H, Hayes SD, Heride C, Rigden DJ, Clague MJ. Systematic survey of deubiquitinase localization identifies USP21 as a regulator of centrosome- and microtubule-associated functions. Mol Biol Cell 2012;23:1095–103.
[27] Clague MJ, Barsukov I, Coulson JM, Liu H, Rigden DJ, Urbe S. Deubiquitylases from genes to organism. Physiol Rev 2013;93:1289–315.
[28] Zaky MY, Liu X, Wang T, Wang S, Liu F, Wang D, et al. Dynasore potentiates c-Met inhibitors against hepatocellular carcinoma through destabilizing c-Met. Arch Biochem Biophys 2020;680:108239.
[29] Row PE, Liu H, Hayes S, Welchman R, Charalabous P, Hofmann K, et al. The MIT domain of UBPY constitutes a CHMP binding and endosomal localization signal required for efficient epidermal growth factor receptor degradation. J Biol Chem 2007;282:30929–37.
[30] Pal A, Young MA, Donato NJ. Emerging potential of therapeutic targeting of ubiquitin-specific proteases in the treatment of cancer. Cancer Res 2014;74:4955–66.
[31] Chen Di, Ning Z, Chen H, Lu C, Liu X, Xia T, et al. An integrative pan-cancer analysis of biological and clinical impacts underlying ubiquitin-specific-processing proteases. Oncogene 2020;39(3):587–602.
[32] Colombo M, Vallese S, Peretto I, Jacq X, Rain J-C, Colland F, et al. Synthesis and biological evaluation of 9-oxo-9H-indeno[1,2-b]pyrazine-2,3-dicarbonitrile analogues as potential inhibitors of deubiquitinating enzymes. ChemMedChem 2010;5(4):552–8.
[33] Sung H, Ferlay J, Siegel RL, Laversanne M, Soerjomataram I, Jemal A, et al. Global Cancer Statistics 2020: GLOBOCAN Estimates of Incidence and Mortality Worldwide for 36 Cancers in 185 Countries. CA A Cancer J Clin 2021;71(3):209–49.
[34] De Toma A, Lo Russo G, Signorelli D, Pagani F, Randon G, Galli G, et al. Uncommon targets in non-small cell lung cancer: Everyone wants a slice of cake. Crit Rev Oncol/Hematol 2021;160:103299. doi: https://doi.org/10.1016/j.critrevonc.2021.103299.
[35] Clague MJ, Urbé S. Endocytosis: the DUB version. Trends Cell Biol 2006;16(11):551–9.
[36] Clague MJ, Coulson JM, Urbe S. Cellular functions of the DUBs. J Cell Sci 2012;125:277–86.
[37] McCullough J, Clague MJ, Urbe S. AMSH is an endosome-associated ubiquitin isopeptidase. J Cell Biol 2004;166:487–92.
[38] Komander D, Clague MJ, Urbé S. Breaking the chains: structure and function of the deubiquitinases. Nat Rev Mol Cell Biol 2009;10(8):550–63.
[39] Islam MT, Chen F, Chen H. The oncogenic role of ubiquitin specific peptidase (USP8) and its signaling pathways targeting for cancer therapeutics. Arch Biochem Biophys 2021;701:108811.
[40] Naviglio S, Mattecucci C, Matoskova B, Nagase T, Nomura N, Di Fiore PP, et al. UBPY: a growth-regulated human ubiquitin isopeptidase. EMBO J 1998;17:3241–50.
[41] Kim Y, Shiba-Ishii A, Nakagawa T, Husni RE, Sakashita S, Takeuchi T, et al. Ubiquitin-specific protease 8 is a novel prognostic marker in early-stage lung adenocarcinoma. Pathol Int 2017;67(6):292–301.
[42] Dufner A, Knobeloch KP. Ubiquitin-specific protease 8 (USP8/UBPy): a prototypic multidomain deubiquitinating enzyme with pleiotropic functions. Biochem Soc Trans 2019;47:1867–79.
[43] Mizuno E, Kobayashi K, Yamamoto A, Kitamura N, Komada M. A deubiquitinating enzyme UBPY regulates the level of protein ubiquitination on endosomes. Traffic 2006;7:1017–31.
[44] Jacomin AC, Fauvarque MO, Taillebourg E. A functional endosomal pathway is necessary for lysosome biogenesis in Drosophila. BMC Cell Biol 2016;17:36.
[45] Colland F. The therapeutic potential of deubiquitinating enzyme inhibitors. Biochem Soc Trans 2010;38:137–43.
[46] D'Arcy P, Wang X, Linder S. Deubiquitinase inhibition as a cancer therapeutic strategy. Pharmacol Ther 2015;147:32–54.